Prediction of source contributions to urban background PM₁₀ concentrations in European cities: a case study for an episode in December 2016 - Part.1 The country contributions

5   Matthieu Pommier[1], Hilde Fagerli[1], Michael Schulz[1], Alvaro Valdebenito[1], Richard Kranenburg[2], Martijn Schaap[2,3]

1 Norwegian Meteorological Institute, Oslo, Norway
2 TNO, PO Box 80015, 3508TA Utrecht, The Netherlands
10 3 FUB – Free University Berlin, Institut für Meteorologie, Carl-Heinrich-Becker-Weg 6-10, 12165 Berlin, Germany

Correspondence to: matthieu.pommier@met.no

Abstract.

A large fraction of the urban population in Europe is exposed to particulate matter levels above the WHO guideline. To make

15 more effective mitigation strategies, it is important to understand the influence on particulate matter (PM) from pollutants

emitted in different European nations. In this study, we evaluate a source apportionment forecasting system aimed to assess

the domestic and transboundary contributions to PM in major European cities for an episode in December 2016. The system

is composed of two models (EMEP/MSC-W rv4.15 and LOTOS-EUROS v2.0) which allows to consider differences in the

source attribution.

20 We also compared the PM₁₀ concentrations and both models present satisfactory agreement in the 4day-forecasts of the surface

concentrations, since the hourly concentrations can be highly correlated with in-situ observations. The correlation coefficients

reach values up to 0.58 for LOTOS-EUROS and 0.50 for EMEP for the urban stations; and 0.58 for LOTOS-EUROS and 0.72

for EMEP for the rural stations. However, the models under-predict the highest hourly concentrations measured by the urban

stations (mean underestimation by 36%), predictable with the relatively coarse model resolution used (0.25° longitude × 0.125°

25 latitude).

For the source receptor calculations, the EMEP/MSC-W model uses a scenario having reduced anthropogenic emissions and

then it is compared to a reference run where no changes are applied. Different percentages (5%, 15% and 50%) in the reduced

emissions were used to test the robustness of the methodology. The impact of the different ways to define the urban area for

the studied cities was also investigated (i.e. 1 model grid cell, 9 grid cells and the grid cells covering the definition given by

30 the Global Administrative Area - GADM). We found that by combining the use of the 15% factor and of a larger domain for

the city edges (9 grid cells or GADM), it helps to reduce the impact of non-linearity on the chemistry which is seen in the

mismatch between the total concentration and the sum of the concentrations from different calculated sources. Even limited,

this non-linearity is observed in the NO_3^-, NH_4^+ and H₂O concentrations, which is related to gas-aerosol partitioning of the

species. The use of a 15% factor and of a larger city domain also gives a better agreement in the determination of the main

35   country contributors between both country source receptor calculations.

During the studied episode, dominated by the influence of the domestic emissions for the 34 European cities investigated and

occurring from December 01st to 09th 2016, the two models agree 68% of the time (on hourly resolution) on the country, having

been the dominant contributor to PM$_{10}$ concentrations. 75% of the hourly predicted PM$_{10}$ concentrations by both models, have

the same top 5 main country contributors. Better results are found in the determination the dominant country contributor for

40   the primary component (70% for POM and 80% for EC) than for the secondary inorganic aerosols (50%).

45

50

55

60

65

1. Introduction.

The adverse health impacts from air pollution and especially from particulate matter (PM) is a well-documented problem (e.g. Keuken et al., 2011; REVIHAAP, 2013; Mukherjee and Agrawal, 2017; Segersson et al., 2017). Furthermore, it affects crops yields (e.g. Crippa et al., 2016), visibility (e.g. Founda et al., 2016) and even the economy (e.g. Meyer and Pagel, 2017). The mass of particulate matter with an aerodynamic diameter lower than 10 µm (PM_{10}) is an air quality metric linked to premature mortality at high exposure (e.g. Dockery and Pope, 1994). The World Health Organization (WHO) states a short-term exposure PM_{10} guideline value of 50 µg/m³ daily mean that should not be exceeded in order to ensure healthy conditions (the long-term exposure guideline is 20 µg/m³ for annual-mean PM_{10}). Although policies have been proposed and implemented at the international (e.g. Amann et al., 2011) and national (e.g.D'Elia et al., 2009) levels, European cities still suffer from poor air quality (EEA report 2017), especially due to high PM_{10} concentrations. In short, to further decrease the adverse health impacts of PM in Europe its concentrations need to be reduced further.

PM_{10} concentrations in the atmosphere are highly variable in space and time. Due to the short atmospheric life time the variability is impacted by local sources, meteorological conditions affecting dispersion and long-range transport as well as chemical regimes controlling the efficiency of secondary formation. PM_{10} consists of both primary and secondary components. Primary PM_{10} components include organic matter (OM), elemental carbon (EC), dust, sea salt (SS) and other compounds. Secondary PM_{10} comprises compounds formed through atmospheric processing of gas-phase precursors. This includes various compounds as nitrate (NO_3^-) from nitrogen oxide (NO_x) emissions, ammonium (NH_4^+) from ammonia (NH_3) emissions, sulphate (SO_4^{2-}) from sulphur dioxide (SO_2) emissions, and a large range of secondary organic aerosol (SOA) compounds from both anthropogenic and biogenic volatile organic compounds (VOCs).The sources for PM and its precursors are multiple but the main anthropogenic sources are the traffic and transport, industries, energy production and agriculture. The main natural sources are composed of biomass burning, mineral dust and sea salt. The main sink is the wet deposition. The dry deposition can also be important and depends on the type of land surface such as grass, tree leaves and others; and on meteorological conditions. With these components deriving from various sources, we understand the importance to reflect properly the source contributions in the modelling for policy support.

Many studies have already focused on source receptor relationships to calculate the transport of atmospheric pollutants, with country-to-country relationships (e.g. EMEP Status Report 1/2018) but also over cities (e.g. Thunis et al., 2016; 2018). However, these studies focus on annual means, whereas information is also required on exposure from episodes which cause short-term limit value exceedances throughout Europe. Source apportionment provides valuable information on the attribution of different sources to PM_{10} concentrations. With a country source calculation, it allows to tackle the emissions from the countries responsible for the air pollution episode. Two distinct methodologies have been compared in this study. Indeed, the country source apportionment presented hereafter is performed by two regional models, the EMEP/MSC-W model (Simpson et al., 2012) and LOTOS-EUROS (Manders et al., 2017).

The calculations provided by the EMEP/MSC-W model, use reduced anthropogenic emission scenario and compare to a reference run where no changes are applied. It is also known as the scenario approach. With a such simulation comparison, the

100   simulation with reduced emissions over a source region allows to highlight the impact of this source on the concentrations over a receptor. Hence, the scenario approach is useful for analyzing the concentration changes due to emission reductions. On the other hand, one simulation per source is needed to calculate the impact of each source, as done on annual means for each country in each EMEP report (e.g. EMEP Status Report 1/2018). The scenario approach may also lead to a non-linearity in the calculated concentrations, i.e. a slight difference between the concentrations over a receptor and the sum of the estimated

105   concentrations from different sources over this same receptor, as shown by Clappier et al. (2017a). LOTOS-EUROS traces the origin of air pollutants throughout a simulation using a labeling approach. The advantage of the labelling technique is the reduction of the computational time, in comparison to the scenario approach. It also quantifies the contribution of an emission source to the concentration of one pollutant at one given location. However, it is not designed to study the impact of emission abatement policies to pollutants concentrations (Clappier et al., 2017b) and only traceable atoms can be used in labeling

110   approach, i.e. only conserved atoms (C, N, S), directly related to emission sources, in their different oxidation states. Thus, for example, the origin of ozone (O_3) cannot be studied, which can be done with the scenario approach. This highlights the importance to estimate the reliability of both methodologies in the attribution of sources to PM_{10} concentrations, e.g. to ensure that the concentrations changes related to the scenario approach are not impacted by the non-linearity and to show that both methodologies present similar results.

115   Both models compose the operational country source receptor (SR) prediction system for the European cities within the Copernicus Atmosphere Monitoring Service (CAMS). This system aims at attributing country contribution to surface PM_{10} in European cities for 4-day forecasts. The objective of this study is to evaluate the robustness of a new system that provides forecasts of source region resolved PM for European cities. The evaluation of the system is focused on an event occurring between the December 01st and 09th 2016, which corresponds to the first event listed from the beginning of the development

120   of our system. To do so, the predicted PM_{10} concentrations are compared with observations. The simulations from both models, for the concentrations and the SR calculations are also inter-compared.

Section 2 describes the country SR system composed by the two models and the experiment. Section 3 describes the studied episode and it presents the evaluation of both predictions in terms of PM_{10} concentrations. The methodology used for the SR calculations by both models is explained in Section 4. Then Section 5 gives an overview of the composition and the origin of

125   PM_{10} over the cities predicted by both models, and the issue regarding the non-linearity in the chemistry related to the EMEP SR calculation. Section 6 is a comparison between the two country SR calculations. Finally, the conclusions are provided in Section 7.

2. Description of the country source apportionment system

2.1. Overview of the system

130   Within CAMS, a country SR product has been developed. This is a new forecasting and near-real time source allocation system for surface PM_{10} concentrations and its different components over all European capitals. The predictions are available online on http://policy.atmosphere.copernicus.eu/DailySourceAllocation.html. The concentrations are calculated over the 28 European Union (EU-28) capitals plus Bern, Oslo and Reykjavik. Forecasts for Barcelona, Rotterdam and Zurich are also provided. In addition to providing information about the air quality over the selected cities by focusing on PM_{10}, this product

135   aims at quantifying the contributions of emissions from different countries in each city (Fig. 1).

The system is composed of predictions from two regional models (the EMEP/MSC-W model and LOTOS-EUROS), using two distinct source apportionment methodologies. The EMEP/MSC-W chemistry transport model (Simpson et al., 2012) has been used for decades to calculate SR relationships between European countries (including Russia) (e.g. EMEP Status Report 1/2018) and the LOTOS-EUROS chemistry transport model (Manders et al., 2017) has also been used in several source

140   apportionment studies over Europe, especially for PM (Hendriks et. al., 2013; 2016; Schaap et al., 2013). Both models are involved in the operational air quality analysis and forecasting for Europe in the CAMS regional ensemble system (Marécal et al., 2015) and for China (Brasseur et al., 2019). For the simplicity of the reading, the EMEP/MSC-W model is hereafter referred to as EMEP model.

Both models are Eulerian models but there are differences between these two models such as the calculation of the planetary

145   boundary layer (PBL) and of the advection, the vertical resolution, the presence of the secondary organic aerosol (included in the EMEP model and not in LOTOS-EUROS), PM_{10} diagnosing particle water explicitly in the EMEP model and not in LOTOS-EUROS, the calculation of the biogenic emissions, the description of the gas-phase chemistry and the treatment of dust (from agriculture and traffic are included in LOTOS-EUROS and not in the EMEP model).

The main details about the models and the experiment are provided in the Table 1 and a more complete description is provided

150   in the following Sections.

2.2. Description of the EMEP model

The EMEP model is a 3-D Eulerian chemistry-transport model described in detail in Simpson et al. (2012). Initially, the model has been aimed at European simulations, even if the model has been used over other regions and at global scale for many years (e.g. Jonson et al., 2010). The EMEP model version rv4.15 has been used here in the forecast mode. The version rv4.15 has

155   been described in Simpson et al. (2017) and references cited therein. The main updates since Simpson et al. (2012) and used in this work, concern a new calculation of aerosol surface area (now based upon the semi-empirical scheme of Gerber, 1985), revised parameterizations of N_2O_5 hydrolysis on aerosols, additional gas-aerosol loss processes for O_3, HNO_3 and HO_2, a new scheme for ship NO_x emissions and the use of a new land-cover (used to calculate biogenic VOC emissions and the dry

deposition) (Simpson et al., 2017). This version is the official EMEP Open Source version that was released in September

160   2017 (Tab. 1)

Vertically, the model uses 20 levels defined as sigma coordinates (Simpson et al., 2012). There are about the 10 lowest model

levels within the PBL (~5 levels below 500 m), and the top of the model domain is at 100 hPa. The PBL height is calculated,

based on the turbulent diffusivity coefficient as described in the EMEP Status Report (2003). The numerical solution of the

advection terms is based upon the scheme of Bott (1989).

165   The chemical scheme couples the sulphur and nitrogen chemistry to the photochemistry using about 140 reactions between 70

species (Andersson-Sköld and Simpson, 1999; Simpson et al. 2012). The chemical mechanism is based on the "EMEP scheme"

described in Simpson et al. (2012) and references therein.

The biogenic emissions of isoprene and monoterpene are calculated in the model by emission factors as a function of

temperature and solar radiation (Simpson et al., 2012).

170   PM emissions are split into EC, OM (here assumed inert) and the remainder, for both fine and coarse PM. The OM emissions

are further divided into fossil-fuel and wood-burning compounds for each source sector. As in Bergström et al. (2012), the

OM/OC ratios of emissions by mass are assumed to be 1.3 for fossil-fuel sources and 1.7 for wood-burning sources. The model

also calculates windblown dust emissions from soil erosion. Secondary aerosol consists of inorganic sulphate, nitrate and

ammonium, and SOA; the latter is generated from both anthropogenic and biogenic emissions, using the 'VBS' scheme

175   detailed in Bergström et al (2012) and Simpson et al. (2012).

The main loss process for particles is wet-deposition, and the model calculates in-cloud and sub-cloud scavenging of gases

and particles as detailed in Simpson et al. (2012). Wet scavenging is treated with simple scavenging ratios, taking into account

in-cloud and sub-cloud processes.

In the EMEP model, the 3D precipitation is needed. An estimation of this 3D precipitation can be calculated by EMEP if this

180   parameter is missing in the meteorological fields. This estimate is derived from large scale precipitation and convective

precipitation. The height of the precipitation is derived from the cloud water. Then, it is defined as the highest altitude above

the lowest level, where the cloud water is larger than a threshold taken as 1.0×10^{-7} kg water per kg air. Precipitations are only

defined in areas where surface precipitations occur. The intensity of the precipitation is assumed constant over all heights were

they are non-zero

185   Gas and particle species are also removed from the atmosphere by dry deposition. This dry deposition parameterization follows

standard resistance-formulations, accounting for diffusion, impaction, interception, and sedimentation.

2.3. Description of LOTOS-EUROS

The LOTOS-EUROS model is an off-line Eulerian chemistry-transport model which simulates air pollution concentrations in the lower troposphere solving the advection-diffusion equation on a regular latitude-longitude-grid with variable resolution over Europe (Manders et al., 2017) (Tab. 1).

The vertical grid is based on terrain following vertical coordinates and extends to 5 km above sea level. The model uses a dynamic mixing layer approach to determine the vertical structure, meaning that the vertical layers vary in space and time. The layer on top of a 25 m surface layer follows the mixing layer height, which is obtained from the European Centre for Medium-Range Weather Forecasts (ECMWF) meteorological input data that is used to force the model. The horizontal advection of pollutants is calculated applying a monotonic advection scheme developed by Walcek and Aleksic (1998).

Gas-phase chemistry is simulated using the TNO CBM-IV scheme, which is a condensed version of the original scheme (Whitten et al, 1980). Hydrolysis of N_2O_5 is explicitly described following Schaap et al. (2004).

LOTOS-EUROS explicitly accounts for cloud chemistry computing sulphate formation as a function of cloud liquid water content and cloud droplet pH as described in Banzhaf et al. (2012). For aerosol chemistry the thermodynamic equilibrium module ISORROPIA2 is used (Fountoukis and Nenes, 2007).

The biogenic emission routine is based on detailed information on tree species over Europe (Schaap et al., 2009). The emission algorithm is described in Schaap et al. (2009) and is very similar to the simultaneously developed routine by Steinbrecher et al. (2009). Dust emissions from soil erosion, agricultural activities and resuspension of particles from traffic are included following Schaap et al. (2009).

As in the EMEP model, the 3D precipitation is needed and cloud liquid water profiles are used to diagnose cloud base height and where below and incloud scavenging takes place. The wet deposition module accounts for droplet saturation following Banzhaf et al. (2012). Dry Deposition fluxes are calculated using the resistance approach as implemented in the DEPAC (DEPosition of Acidifying Compounds) module (van Zanten et al., 2011). Furthermore, a compensation point approach for NH_3 is included in the dry deposition module (Wichink Kruit et al., 2012).

2.4. Description of the experiment

The study focuses on the period from December 01st to 09th 2016. In our system, the forecasts provided by the EMEP model slightly cover a different regional domain than LOTOS-EUROS (Tab. 1). To perform properly the analysis between both models, we have harmonized the use of different parameters as the horizontal resolution (Tab. 1). This harmonization has been revealed important for such comparison and increases the consistency of the model results. The impact of such choices is illustrated for the city definitions, for which subjective choices can be made causing inconsistencies.

An initial spin-up of 10 days was conducted. Both models provide four-day air quality forecasts, and the simulations have been defined as "forecast-cycling experiments", i.e. the predicted fields have been used to initialize successive four-day forecasts (e.g Morcrette et al., 2009). The pollution transport in both models is based on forecasted meteorological fields at 12 UTC

from the previous day, with a 3-hour resolution, calculated by Integrated Forecasting System (IFS) of ECMWF. These

220 forecasted meteorological fields correspond to the fields which were used in the online SR production for these dates. The ECMWF operational system does not archive 3D precipitation forecasts, which is needed by the EMEP model and LOTOS-EUROS as mentioned in Sections 2.2 and 2.3. Therefore, a 3D precipitation estimate is derived from IFS surface variables (large scale and convective precipitations) in the EMEP model and the 3D field is based on the cloud liquid water profile in LOTOS-EUROS.

225 The boundary conditions at 00UTC of the current day from the atmospheric Composition module (C-IFS) have been used. These boundary conditions are specified for ozone (O_3), carbon monoxide (CO), nitrogen oxides (NO and NO_2), methane (CH_4), nitric acid (HNO_3), peroxy-acetyl nitrate (PAN), SO_2, ISOP, ethane (C_2H_6), some VOCs, sea salt, Saharan dust and SO_4. In LOTOS-EUROS, sea salt boundary conditions have not been used as these are shown to be overestimated in comparison with the model. In the EMEP model, the sea salt parameter has been used. This may cause a difference between

230 both models in the estimation of the contribution from sea salt especially for the coastal cities.

Both models use the TNO-MACC emission data set for 2011 on $0.25° \times 0.125°$ (longitude-latitude) resolution (Kuenen et al., 2014, see http://drdsi.jrc.ec.europa.eu/dataset/tno-macc-iii-european-anthropogenic-emissions) and the forest fire emissions are from GFASv1.2 inventory (Kaiser et al., 2012).

Since the study aims to quantify the contributions of long-range transport in each city to the urban background PM_{10}, the effect

235 of the choice of the receptor, i.e. the city domain, has been tested. The city receptor has been defined by three definitions: 1 grid (i.e. $0.25°$ lon $\times 0.125°$ lat, corresponding to the emissions data set resolution), 9 grids and the all the grids covering the administrative area provided by the database of Global Administrative Areas (GADM, https://gadm.org/data.html). This latter is the more precise definition in terms of living area, however it may represent a large region for a definition of a city as shown in Fig. S1 (e.g. London, Nicosia, Riga, Sofia). It is important to explain that this study does not aim to quantify the contribution

240 to PM_{10} at a street scale as done in Kiesewetter et al. (2015) but over the full area defining the cities. The relatively coarse definition of the cities is comparable to the definition used in previous studies as in Thunis et al. (2016) who used an area of 35×35 km² or in Skyllakou et al. (2014) who used a radius of 50 km from the city center.

For the contribution, we also have harmonized the definition of the natural contributions. The natural contributions are defined in this study as the sum of the contributions from sea salt, dust and forest fires, except for the BCs. In LOTOS-EUROS, the

245 natural sources (e.g. dust) coming from the boundaries are classified as BCs and not natural.

3. Evaluation of the predicted surface concentrations during the episode

During December 2016, a PM episode with medium intensity developed across North-Western Europe. As a consequence of a high pressure system over central Europe pollutants concentrations were built up over western Europe (see http://policy.atmosphere.copernicus.eu/reports/CAMSReportDec2016-episode.pdf).

250 The episode was characterized by a high pressure system over central Europe. From December 1st to 2nd, high concentrations were measured and predicted over Paris (Figures 1 & 2). In Figure 2, we can also see from December 3rd to December 8th, that levels of PM_{10} were elevated in Western Europe. Especially on December 6th and 7th, concentrations at some measurement stations in France, Belgium, the Netherlands, Germany and Poland, exceeded the daily limit value of 50 µg/m³ (e.g Fig. S2 – see Section 3.2 for more details about the observations).

255 During the following days relatively stable conditions with slow southerly winds characterized the episode until fronts move into western Europe at the 9th. Large concentrations were also predicted between December 6th and 9th over the Po Valley and over UK on December 6th (Figs. 2 and S2).

3.1. Statistical metric used

To proper estimate the quality of these forecasts, five statistical parameters have been used, such as the Pearson correlation

260 (r), the Mean Bias (MB), the Normalized Mean Bias (NMB), the Root-Mean-Square Error (RMSE) and the Fractional Gross Error (FGE). The ideal score of these parameters is 0 except for the correlation which is 1.

The MB provides the information about the absolute bias of the model, with negative values indicating underestimation and positive values indicating overestimation by the model. The NMB represents the model bias relative to the reference. The RMSE considers error compensation due to opposite sign differences and encapsulates the average error produced by the

265 model. The FGE is a measure of model error, ranging between 0 and 2 and behaves symmetrically with respect to under- and overestimation, without over emphasizing outliers.

We have used M and R as notation to refer, respectively, to model and the reference data (e.g. observations), and N is the number of the reference data set.

Thus MB is calculated by equation (1) and expressed in µg/m³:

$$MB = \frac{\sum_{i=1}^{N}(M_i - R_i)}{N} \qquad (1)$$

270 NMB is calculated by equation (2):

$$NMB = \frac{\sum_{i=1}^{N}(M_i - R_i)}{\sum_{i=1}^{N} R_i} \times 100\% \qquad (2)$$

RMSE is calculated by equation (3) and expressed in µg/m³:

$$RMSE = \sqrt{\frac{\sum_{i=1}^{N}(M_i - R_i)^2}{N}} \qquad (3)$$

and FGE is calculated by equation (4) and dimensionless:

$$FGE = \frac{2}{N} \sum_{i=1}^{N} \frac{|M_i - R_i|}{|M_i + R_i|} \qquad (4)$$

3.2. Comparison with observations

3.2.1. Methodology

275 In order to evaluate the reliability of the predictions, the modelled hourly PM_{10} concentrations have been compared with the AirBase data (see https://acm.eionet.europa.eu/databases/airbase/). The traffic stations were not included in the comparison since a regional model with a somewhat coarse resolution will not be able to calculate enormous concentrations which may be measured by these stations. Indeed, the concentrations calculated by a regional model over cities are mostly representative of the urban background. The observations have also been categorized into two sets of data by differentiating the rural stations

280 to the urban stations (as shown in Fig. S2). This follows the procedure done in the yearly evaluation of the EMEP model over Europe (e.g. EMEP Status Report 1/2018). Due to the relatively coarse definition of a city, it appears that stations classified as rural may be present in our city domain.

It was noticed that for the smaller definition of the city edges, i.e. 1 grid, there were no rural stations within the city domain. Obviously, by increasing the size of the city domain, to 9 grids or by using the GADM definition, the number of rural stations

285 present within the city domain increases. Indeed, all the hourly measurements are averaged within the city edge, by separating the urban and the rural stations. A comparison with these two types of stations can highlight a difference between the urban background and the urban concentrations. For such comparison, the model concentrations are also averaged over the city domain.

3.2.2. Results

290 Figures 3 and 4 show the comparison between the hourly averaged observations within the city edges defined by the 9 grids definition, and the predictions from EMEP and from LOTOS-EUROS respectively.

Figures 3 and 4 show that for the urban stations, the different predictions from a same model, for the same date, are consistent since the values for the statistical parameters are relatively constant. It is noticed; however, that the bias is slightly reduced when the starting date of the forecast is closer to the target date. The available observations and thus the stations may also

295 differ from day to day (e.g. Fig. S2a). Figures 3 and 4 also show that despite many differences, the models have very similar performances in comparison with the urban stations.

In Figure 3, it is also clear that the EMEP model has difficulties to reproduce the highest concentrations measured by the urban stations which are probably smoothed by the model over a large domain as the one defining the cities. This mis-representation of the largest urban concentrations is highlighted by the comparison with the rural stations. This also shows that over the area

300 defining the cities there is a large variability in the measured PM_{10} concentrations and that few stations are not necessarily representative of the model grids. It also shows with such resolution; the model represents urban background concentrations. Only 5 cities have measurements defined as rural stations by using the 9 grids definition (i.e. Amsterdam, Berlin, Luxembourg, Rotterdam and Vienna) while there are up to 19 cities with urban stations. By comparing only, the 5 cities having urban and

rural stations, the agreement between EMEP and the urban stations is largely improved as shown in Fig. S3. We can also notice

305   that the difference in concentrations predicted by the EMEP model between both types of stations is also reduced. This shows

that for these five cities, the predicted PM_{10} concentrations on December 6th are higher than over the other cities.

LOTOS-EUROS has more difficulty to reproduce the hourly variation of the concentrations measured by the rural stations

than EMEP (Fig. 4). However, LOTOS-EUROS also presents an improvement in the bias with these rural stations in

comparison with the urban stations which is predictable since with such resolution, since the model calculates mainly the urban

310   background concentrations. By comparing the 5 cities having urban and rural stations, as done with EMEP, only the bias and

the FGE between the predictions and the measurements with the urban stations are improved (Fig S4). It is also worth noting

that the concentrations predicted by LOTOS-EUROS over these 5 cities are lower than from the EMEP model.

By using the GADM definition, the number of cities having rural stations decreases to 2 while the number of cities with the

urban stations remains identical.

315   Globally, both models present similar performance with the observations especially for the NMB, RMSE and FGE as presented

in Figures S5 and S6. These figures show an overview of the statistical parameters for all 4-d forecast, i.e. the dates from

December 01st to 12th 2016 with a starting date from December 01st to 09th, for all the cities defined by 9 grids, in comparison

with the concentrations measured by the urban and the rural stations, respectively.

As already shown by Figs. 3 and 4, LOTOS-EUROS shows slightly better correlation coefficients with the urban stations than

320   EMEP (Fig. S5, in average $R_{LOTOS-EUROS}$=0.31, R_{EMEP}=0.25; with a maximum of 0.58 for LOTOS-EUROS and 0.5 for EMEP)

and EMEP presents better correlations with the few rural stations (Fig. S6, in average $R_{LOTOS-EUROS}$=0.23, R_{EMEP}=0.35; with a

maximum of 0.58 for LOTOS-EUROS and 0.72 for EMEP). However, the limited number of cities having rural stations

explain the larger variability in the correlations compared to the correlations found with the urban stations. Similar results are

found by using the GADM definition (not shown) while by using only 1 grid to define the city edges, the correlation

325   coefficients with the urban stations are larger (up to 0.8), with an increase in the bias and a decrease in the RMSE (Fig. S7).

In average, both models have a FGE equal to 0.5 over the cities defined by 9 grids with the urban stations and 0.4 with the

rural stations. For the RMSE, it is 33 μg/m^3 with the urban stations and 11 μg/m^3 with the rural stations. While both models

underestimate the PM_{10} concentrations by 36% in average by using the urban sites, EMEP overestimates by 6% with the rural

stations and LOTOS-EUROS underestimates by 6%.

330   Performances of both models are improved with daily means, especially with better correlation coefficients (not shown). For

example, with the cities defined by 9 grids, the correlation coefficients reach 0.8 with the urban stations for EMEP and LOTOS-

EUROS and 0.98 with the rural stations for EMEP. However, a lot of negative correlation coefficients between LOTOS-

EUROS and the rural stations are noticed. Thus, EMEP presents a mean correlation coefficient equal to 0.4 with the urban and

rural stations, and LOTOS-EUROS has a mean correlation of 0.5 with the urban stations and only 0.06 with the rural stations.

335   Better scores with the FGE and the RMSE are also noticed in comparison to the hourly evaluation (not shown). Both models

present with these 9 grids definition a mean FGE of 0.5 with the urban stations and 0.3 for the rural stations and a mean RMSE of 21 μg/m^3 with the urban stations and 10 μg/m^3 with the rural stations.

3.3. Inter-comparison in the concentrations predicted by both models

340 The second analysis has been focused on the agreement between both models. During the episode, all 4-d forecasts present a high correlation between the PM$_{10}$ predicted by the EMEP model and LOTOS-EUROS as shown by Figure 5a. These correlations vary from day to day and city by city but remain large for the different simulated periods (median = 0.7).

There is no clear geographical pattern in terms of performance between the two models, even if the central European cities (e.g. Budapest, Vienna, Warsaw) presented the larger differences (Fig. 5b). These differences may be explained by slightly lower Secondary Inorganic Aerosols (SIA = $NO_3^- + NH_4^+ + SO_4^{2-}$) in LOTOS-EUROS for these cities but also by lack of water 345 in LOTOS-EUROS (which is not diagnosed as mentioned in Sect. 2). Moreover, it confirms the larger PM$_{10}$ concentrations predicted by EMEP than by LOTOS-EUROS for the five cities plotted in Figs. S3 and S4. It is also worth noting that LOTOS-EUROS predicts more sea salt and dust for almost all the cities during the studied period (Fig. S8) which is representative of the overall feature over the regional domain (not shown). Actually it was noticed that for the predicted PM$_{10}$ with the larger positive NMB (EMEP predicting larger PM$_{10}$ concentrations), EMEP has more SIA and "other" than LOTOS-EUROS (Figure 350 S9a), while the PM$_{10}$ from LOTOS-EUROS is dominated by natural components when a larger negative NMB is predicted (Figure. S9b).

4. Methodology of the source receptor calculation

4.1 The EMEP model

4.1.1 Emission reductions

355 The SR calculation follows the methodology uses in each EMEP annual report to quantify the annual country-to-country SR relationships (e.g. EMEP Status Report 1/2018). The experiment is based on a reference run, where all the anthropogenic emissions are included. The other runs are the perturbation runs. These runs correspond to the simulations where the emissions from every considered country are reduced by 15%. As explained in Wind et al. (2004), a reduction by 15% is sufficient to give a clear signal in the pollution changes. It also gives a negligible effect from non-linearity in the chemistry even if in this 360 work it has been estimated.

The perturbation runs are done for emissions of CO, SO$_x$, NO$_x$, NH$_3$, NMVOC and PPM (primary particulate matter). For computational efficiency, in the perturbation calculations, all anthropogenic emissions in the perturbation runs have been reduced here simultaneously. This simultaneous reduction differs from the methodology uses in each EMEP annual report where the emissions are reduced individually.

365   There are in total 31 runs corresponding to the perturbations for each 28 countries from the EU-28, plus Iceland, Norway and

Switzerland, giving the contribution for each country.

To calculate the concentration of the pollutant integrated over the studied area, i.e. a selected city, coming from a source, we

follow the equation (5):

$$C_{source} = \frac{C_{reference} - C_{pertubation}}{x} \qquad (5)$$

With x the reduction factor in % (i.e. 0.15), $C_{reference}$ is the concentration of the pollutant integrated over the studied area from

370   the reference run and $C_{pertubation}$ is the concentration of the pollutant integrated over the studied area from the perturbation run.

The factor x is used to scale the effect of a 15% perturbation to 100%, i.e. an assumed full contribution.

4.1.2 Issue concerning the chemical non-linearity

The reason why emissions should not be perturbed by 100% in the model simulations is to stay within the linear regime of

involved chemistry. Even limited, such methodology may still introduce a non-linearity in the chemistry. The total PM_{10} over

375   the receptor should be identical theoretically to the sum of the PM_{10} originated from the different sources. This is not always

the case and the difference between the total PM_{10} and the sum from the various sources may lead to negative or positive

concentrations. This is a result of the perturbation used which is assumed to be linear to a 100% perturbation.

The 15% factor has been used during many years for the annual country-to-country SR relationships calculations (e.g. EMEP

Status Report 1/2018). Clappier et al. (2017a) have already shown the robustness of the methodology at the country scale on

380   yearly averages and for the highest daily concentrations. However, this factor was not used for smaller areas. Thus this 15%

factor for the study over a city and on hourly basis has been tested, in order to assess the robustness of the calculations. 5%

and 50% were the other selected factors.

Furthermore, by reducing the emissions simultaneously or separately may lead to a slight different result in the concentrations,

but as mentioned previously, this effect is not addressed in this work for computational reason.

385   **4.2. LOTOS-EUROS**

A labelling technique has been developed within each LOTOS-EUROS simulation (Kranenburg et al., 2013). In their study,

Kranenburg et al. (2013) have shown that this technique provides more accurate information about the source contributions

than using a brute force approach with scenario runs as the chemical regime remains unchanged. Another important advantage

is the reduction of computation costs and analysis work associated with the calculations. The source apportionment technique

390   has been previously used to investigate the origin of PM (Hendriks et al., 2013; 2016), NO_2 (Schaap et al., 2013), and nitrogen

deposition (Schaap et al., 2018).

Besides the concentrations of all species the contributions of a number of sources to all components are calculated. The

labelling routine is only implemented for primary, inert aerosol tracers as well as chemically active tracers containing a C, N

395   (reduced and oxidized) or S atom, as these are conserved and traceable. This technique is therefore not suitable to investigate

the origin of e.g. O_3 and H_2O_2, as they do not contain a traceable atom. The source apportionment module for LOTOS-EUROS

provides a source attribution valid for current atmospheric conditions as all chemical conversions occur under the same oxidant

levels. For details and validation of this source apportionment module we refer to Kranenburg et al. (2013).

To avoid violating the memory size and avoid excessive computation times it was chosen to trace the EU-28 countries,

supplemented by Norway and Switzerland. For convenience, a number of small countries was combined with a neighboring

400   state. For example, Switzerland and Liechtenstein as well as Luxembourg and Belgium were combined. In addition, all sea

areas were combined into one source areas. To be mass consistent, all non-specified regions (denoted Rest), natural emissions

and as well as the combined impact of initial conditions and boundary conditions were given labels as well.

5. Information provided by the Source Receptor calculations

5.1 In the EMEP calculations

405   As presented in Fig. 1, the country contributions to the predicted PM_{10} concentrations in the cities is provided in our products.

Figure 6 presents the mean composition for the "Domestic", "30 European countries" and "Others" PM_{10} contributions for all

cities, for all 4-d predictions and split into negative and positive concentrations. The "Domestic" contribution corresponds to

the contribution from the domestic country to the city (for example from France to Paris). The "30 European countries"

corresponds to the other 30 European countries used in the study. "Others" gathers mainly natural sources, the other European

410   countries included in the regional domain (and not included in our SR calculations, e.g. Turkey) and the boundary conditions.

In addition, the impact of the non-linearity has been quantified for each contribution. This figure gives a graphical illustration

of the composition of the different contributions and presents the effect of the non-linearity. Indeed, the positive concentrations

shows the overall composition for each contribution, while the chemical reason of the non-linearity is highlighted by the

negative contribution to the predicted PM_{10} concentrations.

415   For the positive concentrations, a clear feature appears. The main contributors to the "Domestic" PM_{10} are POM (~20%) and

rest PPM (~30%) (which corresponds to the remainder of coarse and fine PPM) (Fig. 6a). Actually, the variation in the mean

concentrations is mainly influenced by the variation in these primary components. NO_3^- is also an important component of

these "Domestic" PM_{10}. The value of the mean concentration depends on the city definition and so on the average of the

concentrations over different size of city. The mean PM_{10} concentration over a smaller area is larger showing that with a smaller

420   grid, the PM_{10} is less diffused over the integrated area. The "30 European countries" PM_{10} is mainly influenced by NO_3^- (by

38%) (Fig. 6b).

Overall, 45% of the contributions to the PM_{10} calculated over the selected cities for this episode are "Domestic" and essentially

due to primary components. 35% are from the "30 European countries", essentially NO_3^- and 25% are from "Others" mainly

composed by natural sources (representing 50% of "Others"). Obviously, this feature is an overview of all selected cities for

425   all the studied dates and it can vary from city to city and from date to date.

By comparing the PM_{10} concentrations calculated over the same city edges but by using different percentages in the perturbation runs, we have calculated the impact of the non-linearity for each contribution. This non-linearity due to the "Domestic" contribution represents in maximum 0.9% of the total PM_{10}. This non-linearity from the "30 European countries" contribution, counts for 0.7% of the total PM_{10} and 1.5% from "Others". Actually, the non-linearity from the "Others" depends

430   on the non-linearity from the two other contributions. This shows that due to the methodology used in the EMEP model, based on a perturbation factor, the non-linearity in the chemistry has a limited impact on the SR calculation. This non-linearity is slightly reduced by using the larger domains to define the cities (e.g. 9 grids). This is also shows that the responses to perturbation runs are robust.

Negligible negative contributions have been calculated for the "Domestic" and "30 European countries" contributions (Figs.

435   6a & b) and small negative contributions are predicted in "Others" (Fig. 6c). These negative PM_{10} are a result of negative values in NO_3^-, NH_4^+ and H_2O which is a consequence of gas-aerosol partitioning of the species. Indeed, NH_3 reacts with nitric acid (HNO_3) to form ammonium nitrate (NH_4NO_3). This is an equilibrium reaction, and thus the transition from solid to gaseous phase depend on relative humidity (e.g. Fagerli and Ass, 2008; Pakkanen, 1996). This shows that, for example, a reduction in NO_x over a country which impacts the selected city, does not necessarily only impact the NO_3^- over this city, but may also

440   have an effect on NH_3 chemistry over a second region. This second region may also have itself an impact on the selected city. This combination of NO_x and NH_3 chemistry from different regions may lead at the end to these negative concentrations.

The impact of the percentage used in the perturbation runs and the size of the city edges have no significant impact in the amount of negative "Others" PM_{10} concentrations. The impact of both parameters is more visible on the "Domestic" and "Rest of Europe" concentrations but it remains very small.

445   The use of larger grids reduces the amount of the negative PM_{10} concentrations and reduces globally the non-linearity. The 15% factor also reduces the negative non-linearity in the "Domestic" concentrations (e.g. H_2O for the 9 grids and GADM runs).

5.2 In the LOTOS-EUROS calculations

As presented with the EMEP predictions, Figure 7 presents the mean composition for the "Domestic", "30 European countries"

450   and "Others" PM_{10} contributions for all cities, for all 4-d predictions provided by LOTOS-EUROS. The definition of "Others" is slightly different than the EMEP one since e.g. the dust from agriculture and traffic is included (see Sect. 2). For an easier comparison, the result for the EMEP model using the 15% factor has also been plotted with thinner charts, even if, as just mentioned, the definition of "Others" slightly differs between both models.

First of all, during the episode, LOTOS-EUROS confirms the global feature calculated by the EMEP model, i.e. the dominant

455   contribution to the surface PM$_{10}$ is "Domestic", ranging between 40% and 48% of the predicted PM$_{10}$ over all selected cities

and for all the studied dates. However, LOTOS-EUROS always presents more "Domestic" PM$_{10}$ than the EMEP model.

LOTOS-EUROS also predicted slightly more influence from "Others" than the "30 European countries" with a ratio close to

25-30% each at the opposite of the EMEP model.

As with the EMEP model, the mean PM$_{10}$ concentration over the smaller city definition is larger and the "Domestic" PM$_{10}$ is

460   largely driven by POM. "Rest", which corresponds to the difference between the total PM$_{10}$ and the sum of all the components,

is also a large component of this "Domestic" PM$_{10}$. POM and "Rest" represent each between 25% and 30% of these "Domestic"

PM$_{10}$.

The large influence of NO_3^- (48%) in the "30 European countries" PM$_{10}$ is also calculated by LOTOS-EUROS, as well as the

large contribution of the natural components (60%) in "Others". It is noteworthy to see that, even small, the dust emitted by

465   the road traffic and the agriculture is not negligible in these "Others" PM$_{10}$ (~10%).

6. Comparison between both country source receptor calculations

Section 3 has highlighted the similar performance from both models in the prediction of the PM$_{10}$ concentrations over the

European cities with observations and Section 5 has shown similar results in terms of composition of these PM$_{10}$. It is also

noteworthy to see in Figure 8 that both SR calculations present a high rate of agreement over the selected period with the

470   common simulated components and the PM$_{10}$ calculated by both models. Indeed, both models show that, by using the 9 grids

definition, 68% of the hourly predicted PM$_{10}$ concentrations have the same dominant country contributor. In average, 50% of

the secondary inorganic aerosols predicted by both models over all the cities and all 4day-forecasts have the same main

contributor. This value goes up to 70% for POM and 80% for EC. For the two primary components (POM and EC) the median

is larger, with a value of 77% and 93% respectively, showing that the mean value in the agreement for both compounds are

475   biased lower by a few low values (Fig. 8). On a daily basis, the mean agreement is slightly improved, e.g. 70% of agreement

for the PM$_{10}$ (Fig. S10). The main improvement is calculated for EC, with a median equal to 100% (Fig. S10).

The lower agreement for the SIA is predictable due to the various origins (chemistry and primary emissions) for these

particulates and the different aerosols treatment (gas-aerosols partitioning) in both models. This agreement varies from city to

city (Fig. 9) but it is shown, in addition to the example of PM$_{10}$ (Fig. 5), that central European cities often present a limited

480   agreement due to their central location and the influence of various countries. This limited agreement is also sometimes

observable for the cities close to the edge of the regional domain (Fig. 9), which could be explained by the influence of the

boundary conditions as the dust transported from other regions (e.g. Valetta influenced by dust from Sahara).

The mean agreement increases up to 75% for determination in the top 5 of the main country contributors to PM$_{10}$ (Fig 10).

This ratio is around 70% for SO_4^{2-}, EC and POM and close to 60% for NO_3^- and equal to 65% for NH_4^+ (Fig. 10). As for the

485 dominant country contributor, the agreement is slightly improved by using daily means, e.g. we found 76% of agreement with

the PM$_{10}$ (not shown).

It is also important to notice that these overall agreements are neither significantly influenced by the definition of the cities

area nor on the perturbation percentage tested for the EMEP SR calculations (Fig. S11). The agreement is slightly better by

using the smaller area (1 grid) in the determination of the dominant country contributor and slightly better by using a large

490 domain (9 grids or GADM) in the determination of the 2 and 5 main contributors.

Overall, a perturbation run using a factor of 15% and the use of a larger city area (e.g. GADM or 9 grids) allow a better

determination in the country contributors, with a better agreement with LOTOS-EUROS and limit the impact of the non-

linearity in the chemistry.

7. Conclusions

495 By focusing on a specific event, occurring from December 01st to 09th 2016 over Europe, this work is the first attempt to

evaluate the source receptor calculations provided by two regional models (EMEP and LOTOS-EUROS) in a forecast mode.

Together, the models compose the operational source receptor prediction system for the European cities within the Copernicus

Atmosphere Monitoring Service (CAMS) and aim to estimate the impact of the long-range transport to urban PM$_{10}$. These

models also use two distinct source apportionment methodologies, a labeling technique for LOTOS-EUROS and the use of

500 perturbation runs for EMEP.

The methodology used for the EMEP model was tested by using three different percentages (5%, 15% and 50%) in the

perturbation runs. The importance in the choice of the domain defining the edges of the studied cities was also investigated in

terms of predicted concentrations and calculated contributors. It was concluded that the 15% factor and the use of large city

areas (9 grids or GADM) were the more efficient. It reduces the impact of non-linearity, which especially impacts the NO_3^-,

505 NH_4^+ and H$_2$O concentrations, and it presents a better agreement in the determination of main country contributors. This non-

linearity always represents less than 2% of the total modelled PM$_{10}$ for each contribution calculated by the EMEP SR and is

caused by the perturbation used which is assumed to be linear to a 100% perturbation.

The predicted PM$_{10}$ concentrations were compared with AirBase observations showing fair agreement even if the models

remain perfectible since they have difficulties to reproduce the highest hourly concentrations measured by the urban stations

510 (mean underestimation by 36%). It was also noticed the bias is slightly reduced when the forecast is closer to the studied date.

An inter-comparison between both models was also performed showing satisfactory results with few discrepancies in the

predictions of the PM$_{10}$ concentrations, mainly explained by an underestimation in sea salt and dust by the EMEP model

(compared to LOTOS-EUROS); and differences in SIA, caused by different chemical aerosols treatment in both models.

During the episode, both model have shown that 45% of the predicted PM$_{10}$ over the selected cities were from "Domestic"

515 sources and essentially composed of primary components. The rest of the contribution was roughly equitably split into an

influence from the others 30 countries used in the regional domain, essentially composed of NO_3^- and from "Others" mainly composed of natural sources.

It was shown that the results from both source apportionment methodologies agree in average by 68% in the determination the dominant country contributor to the hourly PM_{10} concentrations and 75% for the top 5 of these country contributors. The daily

520   country attribution also presents similar agreement.

A full year of evaluation will be necessary to confirm our satisfactory results. Moreover, the bias of the predicted PM_{10} concentrations with the urban observations probably foresees an underestimation of the "Local" contribution (from the city) which is also predicted by the EMEP model. This is investigated in a companion paper (in preparation), also focusing on the same event.

525

Data availability

The EMEP model is an open source model available on https://github.com/metno/emep-ctm. LOTOS-EUROS is an open-source model available on https://lotos-euros.tno.nl/.

Author contribution

530   MP, HF and M Schulz designed the research. MP performed the experiment. MP developed the analyzing codes and analyzed the data. AV developed the EMEP part of the forecasting system. RK and M Schaap performed and provided the LOTOS-EUROS results. MP wrote the paper with the inputs from all coauthors.

Acknowledgments

This work is partly funded by the EU Copernicus project CAMS 71 to provide policy support. This work has also received

535   support from the Research Council of Norway (Programme for Supercomputing) through the EMEP project (NN2890K) for CPU and the Norstore project "European Monitoring and Evaluation Programme" (NS9005K) for storage. The EMEP project itself is supported by the Convention on the Long Range Transmission of Air Pollutants, under UN-ECE. The authors thank A. Mortier (Norwegian Meteorological Institute) for the development and the design of the website (http://policy.atmosphere.copernicus.eu/DailySourceAllocation.html).

540

545 **References**

Amann, M., Bertok, I., Borken-Kleefeld, J., Cofala, J., Heyes, C., Höglund-Isaksson, L., Klimont, Z., Nguyen, B., Posch, M., Rafaj, P., Sandler, R., Schöpp, W., Wagner, F., Winiwarter, W.: Cost-effective Control of Air Quality and Greenhouse Gases in Europe: Modeling and Policy Applications, 26 ,1489-1501, 2011.

550 Andersson-Sköld, Y. and Simpson, D.: Comparison of the chemical schemes of the EMEP MSC-W and the IVL photochemical trajectory models, Atmos. Env., 33(7), 1111-1129, doi:10.1016/S1352-2310(98)00296-9, 1999.

Banzhaf, S., Schaap, M., Kerschbaumer, A., Reimer, E., Stern, R., van der Swaluw, E., Builtjes, P.: Implementation and evaluation of pH-dependent cloud chemistry and wet deposition in the chemical transport model REM-Calgrid. Atmos. Env., 555 49, 378–390, doi:10.1016/j.atmosenv.2011.10.069, 2012.

Bergström, R., Denier van der Gon, H. A. C., Prévôt, A. S. H., Yttri, K. E., and Simpson, D.: Modelling of organic aerosols over Europe (2002–2007) using a volatility basis set (VBS) framework: application of different assumptions regarding the formation of secondary organic aerosol, Atmos. Chem. Phys., 12, 8499-8527, https://doi.org/10.5194/acp-12-8499-2012, 560 2012.

Binkowski, F. S., and Shankar, U.: The Regional Particulate Matter Model 1. Model description and preliminary results, J. Geophys.Res., 100(D12), 26,191–26,209, doi:10.1029/95JD02093, 1995.

565 Bott, A.: A positive definite advection scheme obtained by nonlinear renormalization of the advective fluxes, Mon. Weather Rev.,117(5), 1006-1016, doi:10.1175/1520-0493(1989)117(1006:APDASO)2.0.CO;2, 1989.

Brasseur, G. P., Xie, Y., Petersen, A. K., Bouarar, I., Flemming, J., Gauss, M., Jiang, F., Kouznetsov, R., Kranenburg, R., Mijling, B., Peuch, V.-H., Pommier, M., Segers, A., Sofiev, M., Timmermans, R., van der A, R., Walters, S., Xu, J., and Zhou, 570 G.: Ensemble forecasts of air quality in eastern China – Part 1: Model description and implementation of the MarcoPolo– Panda prediction system, version 1, Geosci. Model Dev., 12, 33-67, https://doi.org/10.5194/gmd-12-33-2019, 2019.

Callaghan, A., de Leeuw, G., Cohen, L., and O'Dowd, C. D.: Relationship of oceanic whitecap coverage to wind speed and wind history, Geophys. Res. Lett., 35, L23609, https://doi.org/10.1029/2008GL036165, 2008.

575

Clappier, A., Fagerli, H., Thunis, P.: Screening of the EMEP source receptor relationships: application to five European countries, Air Qual. Atmos. Health, 10, 4, 497-507, DOI: 10.1007/s11869-016-0443-y, 2017a.

Clappier, A., Belis, C. A., Pernigotti, D., and Thunis, P.: Source apportionment and sensitivity analysis: two methodologies with two different purposes, Geosci. Model Dev., 10, 4245-4256, https://doi.org/10.5194/gmd-10-4245-2017, 2017b.

Crippa, M., Janssens-Maenhout, G., Dentener, F., Guizzardi, D., Sindelarova, K., Muntean, M., Van Dingenen, R., and Granier, C.: Forty years of improvements in European air quality: regional policy-industry interactions with global impacts, Atmos. Chem. Phys., 16, 3825-3841, https://doi.org/10.5194/acp-16-3825-2016, 2016.

Dockery, D. W. and Pope III, C. A.: "Acute respiratory effects of particulate air pollution", Ann. Rev. Public Health, 15, 107-132, DOI: 10.1146/annurev.pu.15.050194.000543, 1994.

D'Elia, I., Bencardino, M., Ciancarella, L., Contaldi, M., Vialetto, G.:Technical and Non-Technical Measures for air pollution emission reduction: The integrated assessment of the regional Air Quality Management Plans through the Italian national model, Atmos. Env., 43, 6182-6189, https://doi.org/10.1016/j.atmosenv.2009.09.003, 2009.

EEA Report No 13/2017, Air quality in Europe 2017, https://www.eea.europa.eu/publications/air-quality-in-europe-2017

EMEP Status Report 1/2003: "Transboundary acidification and eutrophication and ground level ozone in Europe: Unified EMEP model description", The Norwegian Meteorological Institute, Oslo, Norway, ISSN 0806-4520, 2003.

EMEP Status Report 1/2018: "Transboundary particulate matter, photo-oxidants, acidifying and eutrophying components", Joint MSC-W & CCC & CEIP Report, ISSN 1504-6109, 2018.

Fagerli, H. and Aas, W.: Trends of nitrogen in air and precipitation: Model results and observations at EMEP sites in Europe, 1980–2003, Env. Poll., 154, 3, 448-461, https://doi.org/10.1016/j.envpol.2008.01.024, 2008.

Founda, D., Kazadzis, S., Mihalopoulos, N., Gerasopoulos, E., Lianou, M., and Raptis, P. I.: Long-term visibility variation in Athens (1931–2013): a proxy for local and regional atmospheric aerosol loads, Atmos. Chem. Phys., 16, 11219-11236, https://doi.org/10.5194/acp-16-11219-2016, 2016.

Fountoukis, C. and Nenes, A.: ISORROPIA II: a computationally efficient thermodynamic equilibrium model for K^+–Ca^{2+}–Mg^{2+}–NH_4^+–Na^+–SO_4^{2-}–NO_3^-–Cl^-–H_2O aerosols, Atmos. Chem. Phys., 7, 4639-4659, https://doi.org/10.5194/acp-7-4639-2007, 2007.

Gerber, H. E.: Relative-Humidity Parameterization of the Navy Aerosol Model (NAM), Naval Research Laboratory, NRL report 8956, 1985.

Hendriks, C., Kranenburg, R., Kuenen, J., van Gijlswijk, R., Wichink Kruit, R., Segers, A., Denier van der Gon, H., Schaap, M.: The origin of ambient particulate matter concentrations in the Netherlands, Atmos. Env., 69, 289–303, doi:10.1016/j.atmosenv.2012.12.017, 2013.

Hendriks, C., Kranenburg, R., Kuenen, J.J.P., Van den Bril, B., Verguts, V., Schaap, M.: Ammonia emission time profiles based on manure transport data improve ammonia modelling across north western Europe. Atmos. Environ. 131, 83–96, doi:10.1016/j.atmosenv.2016.01.043, 2016.

Jonson, J. E., Stohl, A., Fiore, A. M., Hess, P., Szopa, S., Wild, O., Zeng, G., Dentener, F. J., Lupu, A., Schultz, M. G., Duncan, B. N., Sudo, K., Wind, P., Schulz, M., Marmer, E., Cuvelier, C., Keating, T., Zuber, A., Valdebenito, A., Dorokhov, V., De Backer, H., Davies, J., Chen, G. H., Johnson, B., Tarasick, D. W., Stübi, R., Newchurch, M. J., von der Gathen, P., Steinbrecht, W., and Claude, H.: A multi-model analysis of vertical ozone profiles, Atmos. Chem. Phys., 10, 5759-5783, doi:10.5194/acp-10-5759-2010, 2010.

Kaiser, J. W., Heil, A., Andreae, M. O., Benedetti, A., Chubarova, N., Jones, L., Morcrette, J.-J., Razinger, M., Schultz, M. G., Suttie, M., and van der Werf, G. R.: Biomass burning emissions estimated with a global fire assimilation system based on observed fire radiative power, Biogeosciences, 9, 527-554, https://doi.org/10.5194/bg-9-527-2012, 2012.

Keuken, M, Zandveld, P., van den Elshout, S., Janssen, N. A. H., Hoek, G.: Air quality and health impact of PM_{10} and EC in the city of Rotterdam, the Netherlands in 1985–2008. Atmos Env., 45, 5294–5301, doi:10.1016/j.atmosenv.2011.06.058, 2011.

Kiesewetter, G., Borken-Kleefeld, J., Schöpp, W., Heyes, C., Thunis, P., Bessagnet, B., Terrenoire, E., Fagerli, H., Nyiri, A., and Amann, M.: Modelling street level PM_{10} concentrations across Europe: source apportionment and possible futures, Atmos. Chem. Phys., 15, 1539-1553, https://doi.org/10.5194/acp-15-1539-2015, 2015.

640   Kranenburg, R., Segers, A. J., Hendriks, C., and Schaap, M.: Source apportionment using LOTOS-EUROS: module
      description and evaluation, Geosci. Model Dev., 6, 721-733, https://doi.org/10.5194/gmd-6-721-2013, 2013.

      Kuenen, J. J. P., Visschedijk, A. J. H., Jozwicka, M., and Denier van der Gon, H. A. C.: TNO-MACC_II emission inventory;
      a multi-year (2003–2009) consistent high-resolution European emission inventory for air quality modelling, Atmos. Chem.
645   Phys., 14, 10963-10976, https://doi.org/10.5194/acp-14-10963-2014, 2014.

      Manders, A. M. M., Builtjes, P. J. H., Curier, L., Denier van der Gon, H. A. C., Hendriks, C., Jonkers, S., Kranenburg, R.,
      Kuenen, J. J. P., Segers, A. J., Timmermans, R. M. A., Visschedijk, A. J. H., Wichink Kruit, R. J., van Pul, W. A. J., Sauter,
      F. J., van der Swaluw, E., Swart, D. P. J., Douros, J., Eskes, H., van Meijgaard, E., van Ulft, B., van Velthoven, P., Banzhaf,
650   S., Mues, A. C., Stern, R., Fu, G., Lu, S., Heemink, A., van Velzen, N., and Schaap, M.: Curriculum vitae of the LOTOS–
      EUROS (v2.0) chemistry transport model, Geosci. Model Dev., 10, 4145-4173, https://doi.org/10.5194/gmd-10-4145-2017,
      2017.

      Marécal, V., Peuch, V.-H., Andersson, C., Andersson, S., Arteta, J., Beekmann, M., Benedictow, A., Bergström, R., Bessagnet,
655   B., Cansado, A., Chéroux, F., Colette, A., Coman, A., Curier, R. L., Denier van der Gon, H. A. C., Drouin, A., Elbern, H.,
      Emili, E., Engelen, R. J., Eskes, H. J., Foret, G., Friese, E., Gauss, M., Giannaros, C., Guth, J., Joly, M., Jaumouillé, E., Josse,
      B., Kadygrov, N., Kaiser, J. W., Krajsek, K., Kuenen, J., Kumar, U., Liora, N., Lopez, E., Malherbe, L., Martinez, I., Melas,
      D., Meleux, F., Menut, L., Moinat, P., Morales, T., Parmentier, J., Piacentini, A., Plu, M., Poupkou, A., Queguiner, S.,
      Robertson, L., Rouïl, L., Schaap, M., Segers, A., Sofiev, M., Tarasson, L., Thomas, M., Timmermans, R., Valdebenito, Á.,
660   van Velthoven, P., van Versendaal, R., Vira, J., and Ung, A.: A regional air quality forecasting system over Europe: the MACC-
      II daily ensemble production, Geosci. Model Dev., 8, 2777-2813, https://doi.org/10.5194/gmd-8-2777-2015, 2015.

      Mårtensson, E.M., Nilsson, E.D., de Leeuw, G., Cohen, L.H. and Hansson, H.C.: Laboratory simulations and parameterization
      of the primary marine aerosol production. J. Geophys. Res. Atmos., 108., D9, 4297, doi:10.1029/2002JD002263,2003.
665
      Meyer, S. and Pagel, M.: Fresh Air Eases Work - The Effect of Air Quality on Individual Investor Activity, NBER Working
      Paper No. 24048, DOI: 10.3386/w24048, 2017.

      Monahan, E., Spiel, D., and Davidson, K.: A model of marine aerosol generation via white caps and wave disruption, in:
670   Oceanic whitecaps, edited by: Monahan, E. and MacNiochaill, G., 167–193, Dordrecht: Reidel, The Netherlands, 1986.

Morcrette, J.-J, Boucher, O., Jones, L., Salmond, D., Bechtold, P., Beljaars, A., Benedetti, A., Bonet, A., Kaiser, J. W., Razinger, M., Schulz, M., Serrar, S., Simmons, A. J., Sofiev, M., Suttie, M., Tompkins, A. M., Untch, A.: Aerosol analysis and forecast in the ECMWF Integrated Forecast System: Forward modeling, J. Geophys. Res., 114, D06206, doi:10.1029/2008JD011235, 2009.

Mukherjee, A., and Agrawal, M.: World air particulate matter: sources, distribution and health effects, Environmental Chemistry Letters, 15, 2,283-309, DOI: 10.1007/s10311-017-0611-9, 2017.

Pakkanen, T. A.: Study of formation of coarse particle nitrate aerosol, Atmos. Env., 30, 2475-2482, doi: 1352-2310(95)00492-0, 1996

REVIHAAP, Review of Evidence on Health Aspects of Air Pollution - REVIHAAP Project Technical Report, World Health Organization (WHO) Regional Office for Europe, Bonn, 2013, http://www.euro.who.int/__data/assets/pdf_file/0004/193108/REVIHAAP-Final-technical-report-final-version.pdf

Schaap, M., van Loon, M., ten Brink, H. M., Dentener, F. J., and Builtjes, P. J. H.: Secondary inorganic aerosol simulations for Europe with special attention to nitrate, Atmos. Chem. Phys., 4, 857-874, https://doi.org/10.5194/acp-4-857-2004, 2004.

Schaap, M., Manders, A. M. M., Hendriks, E. C. J., Cnossen, J. M., Segers, A. J. S., Denier van der Gon, H. A. C., Jozwicka, M., Sauter, F. J., Velders, G. J. M., Matthijsen J., and Builtjes, P.J.H. : Regional modelling of particulate matter for the Netherlands, PBL-rapport 500099008, Den Haag/Bilthoven: PBL, 2009.

Schaap, M., Kranenburg, R., Curier, L., Jozwicka, M., Dammers, E., and Timmermans, R.: Assessing the Sensitivity of the OMI-NO$_2$ Product to Emission Changes across Europe, Remote Sens. 5, 4187–4208, doi:10.3390/rs5094187, 2013.

Schaap, M., Hendriks, C., Kranenburg, R., Kuenen, J., Segers, A., Schlutow, A., Nagel, H.-D., Ritter, A., and Banzhaf, S.: PINETI-III: Modellierung und Kartierung atmosphäri-scher Stoffeinträge von 2000 bis 2015 zur Bewer-tung der ökosystem-spezifischen Gefährdung von Biodiversität in Deutschland. UBA-Texte. Retrieved from https://gis.uba.de/website/depo1/download/PINETI-3_Abschlussbericht_fuer_mapserver_vorl.pdf, 2018.

Segersson, D., Eneroth, K., Gidhagen, L., Johansson, C., Omstedt, G., Engström Nylén, A. and Forsberg, B.: Health Impact of PM_{10}, $PM_{2.5}$ and Black Carbon Exposure Due to Different Source Sectors in Stockholm, Gothenburg and Umea, Sweden, Int. J. Environ. Res. Public Health, 14(7), 742; doi:10.3390/ijerph14070742, 2017.

705

Simpson, D., Benedictow, A., Berge, H., Bergström, R., Emberson, L. D., Fagerli, H., Flechard, C. R., Hayman, G. D., Gauss, M., Jonson, J. E., Jenkin, M. E., Nyíri, A., Richter, C., Semeena, V. S., Tsyro, S., Tuovinen, J.-P., Valdebenito, Á., and Wind, P.: The EMEP MSC-W chemical transport model – technical description, Atmos. Chem. Phys., 12, 7825-7865, https://doi.org/10.5194/acp-12-7825-2012, 2012.

710

Simpson, D., Bergström, R., Imhof, H., and Wind, P.: Updates to the EMEP/MSC-W model, 2016-2017 Transboundary particulate matter, photo-oxidants, acidifying and eutrophying components. EMEP Status Report 1/2017, The Norwegian Meteorological Institute, Oslo, Norway, 15-36, ISSN 1504-6109, 2017.

715 Skyllakou, K., Murphy, B. N., Megaritis, A. G., Fountoukis, C., and Pandis, S. N.: Contributions of local and regional sources to fine PM in the megacity of Paris, Atmos. Chem. Phys., 14, 2343-2352, https://doi.org/10.5194/acp-14-2343-2014, 2014.

Steinbrecher, R., Smiatek, G., Köble, R., Seufert, G., Theloke, J., Hauff, K., Ciccioli, P., Vautard, R., Curci, G.: 2009. Intra- and inter-annual variability of VOC emissions from natural and semi-natural vegetation in Europe and neighbouring countries.
720 Atmos. Env., 43, 1380–1391, doi:10.1016/j.atmosenv.2008.09.072, 2009.

Thunis, P., Degraeuwe, B., Pisoni, E., Ferrari, F., Clappier, A.:On the design and assessment of regional air quality plans: The SHERPA approach, J. Env. Management, 183, 952-958, http://dx.doi.org/10.1016/j.jenvman.2016.09.049, 2016.

725 Thunis, P., Degraeuwe, B., Pisoni, E., Trombetti, M., Peduzzi, E., Belis, C. A., Wilson, J., Clappier, A., Vignati, E.: $PM_{2.5}$ source allocation in European cities: A SHERPA modelling study, Atmos. Env., 187, 93-106, doi.org/10.1016/j.atmosenv.2018.05.062, 2018.

Tuovinen, J.-P., Ashmore, M. R., Emberson, L. D., Simpson, D.: Testing and improving the EMEP ozone deposition module,
730 Atmos. Env., 38, 2373-2385, https://doi.org/10.1016/j.atmosenv.2004.01.026, 2004.

Van Zanten, M. C., Sauter, F. J., Wichink Kruit, R. J., Van Jaarsveld, J. A., and Van Pul, W. A. J.: Description of the DEPAC module: Dry deposition modelling with DEPAC GCN2010, RIVM report 680180001/2010, Bilthoven, the Netherlands, 74., 2010.

735

Walcek, C. J. and Aleksic, N. M.: A simple but accurate mass conservative peak-preserving, mixing ratio bounded advection algorithm with fortran code, Atmos. Environ., 32, 3863–3880, https://doi.org/10.1016/S1352-2310(98)00099-5, 1998.

Wichink Kruit, R. J., Schaap, M., Sauter, F. J., van Zanten, M. C., and van Pul, W. A. J.: Modeling the distribution of ammonia

740   across   Europe   including   bi-directional   surface–atmosphere   exchange,   Biogeosciences,   9,   5261-5277, https://doi.org/10.5194/bg-9-5261-2012, 2012.

Whitten, G., Hogo, H., Killus, J.: The carbon bond mechanism for photochemical smog, Environ. Sci. Technol., 14 (6), 690– 700, DOI: 10.1021/es60166a008, 1980.

745

Wind, P., Simpson, D., Tarrasón, L.: Chap. 4 Source-receptor calculations, EMEP Status Report 1/2004: "Transboundary acidification, eutrophication and ground level ozone in Europe", Joint MSC-W & CCC & CIAM & ICP-M&M & CCE Report, ISSN 0806-4520, 2004.

750   Zhang, L., Gong, S., Padro, J., and Barrie, L.: A size-segregated particle dry deposition scheme for an atmospheric aerosol module, Atmos. Env., 35, 549–560, https://doi.org/10.1016/S1352-2310(00)00326-5, 2001.

755

760

Table. 1 Technical description of both models used in the SR calculation system.

Model	EMEP/MSC-W	LOTOS-EUROS
Model version	rv4.15 (open source version Sept 2017)	V2.0 (open source version 2016)
Horizontal resolution	$0.25° \times 0.125°$ lon-lat	$0.25° \times 0.125°$ lon-lat
Regional domain	30°N-76°N 30°W-45°E	31°N-68.875°N 24°W-43.75°E
PBL	Calculation based on turbulent diffusion coefficients (Kz) (EMEP Status Report 1/2003)	From ECMWF
Vertical resolution	20 sigma layers up to 100 hPa, with about 10 in the Planetary Boundary Layer	Mixing layer approach with a 25m surface layer. Model top at 5 km.
Gas phase chemistry	Evolution of the "EMEP scheme" (Andersson-Sköld and Simpson, 1999; Simpson et al. 2012)	TNO-CBM-IV (Schaap et al., 2009)
Nitrate formation	Oxidation of NO_2 by O_3 on aerosols (night and winter) N_2O_5 hydrolysis on aerosol (Simpson et al., 2012)	N_2O_5 hydrolysis on aerosol (Schaap et al., 2004)
Sulphate production	SO_2 oxidation by O_3 and H_2O_2	SO_2 oxidation by O_3 and H_2O_2
Inorganic aerosols	MARS (Binkowski and Shankar, 1995)	ISORROPIA-II (Fountoukis and Nenes, 2007)
Secondary organic aerosols	EmChem09soa (Bergström et al, 2012)	Not included in this model version
Water	PM_{10} particle water at 50% relative humidity	Not diagnosed
Advection	Scheme of Bott (1989)	Monotonic advection scheme (Walceck and Aleksic, 1998)
Dry deposition/sedimentation	Resistance approach for gases and for aerosol, including non-stomatal deposition of NH_3 (EMEP Status Report 1/2003)	Resistance approach for gases and for aerosol, including compensation point for NH_3 (van Zanten et al., 2011; Wichnik Kuit et al., 2012; Zhang, 2001)
Wet deposition	wash out ratio's	pH dependent wash out ratio's accounting for saturation
Dust	Boundary conditions + windblown dust	Boundary conditions + Soil, traffic and agriculture (Schaap et al., 2009)
Sea Salt	Mårtensson et al. (2003), Monahan (1986) production accounting for whitecap area fractions (Callaghan et al., 2008)	Mårtensson et al. (2003), Monahan (1986)
Boundary values	global C-IFS 00UTC	global C-IFS 00UTC, except for sea salt
Initial values	24h forecast from the day before	24h forecast from the day before
Anthropogenic emissions	TNO-MACC-III for 2011	TNO-MACC-III for 2011
Fire emissions	CAMS product: GFAS	CAMS product: GFAS

Biogenic emissions	Emission factors as a function of temperature and solar radiation (Simpson et al., 2012)	Emission factors as a function of temperature and solar radiation (Schaap et al., 2009)
Meteorological driver	12:00 UTC operational IFS forecast (yesterday's)	12:00 UTC operational IFS forecast (yesterday's)

765
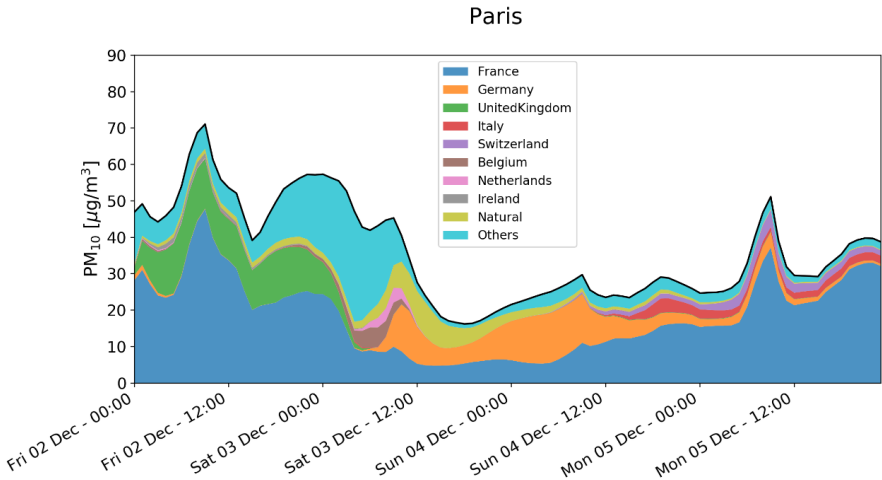
Figure 1: Hourly PM$_{10}$ concentrations in µg/m^3 over Paris predicted by the EMEP model from December 2nd to December 5th 2016. The black curve highlights the total concentration. The eight main country contributors are plotted in addition to the natural sources and "Others". "Others" gathers hereafter other European countries, the boundary conditions, the ship traffic, the biogenic sources, the soil NO emission, the aircraft emission and the lightning.

770

775
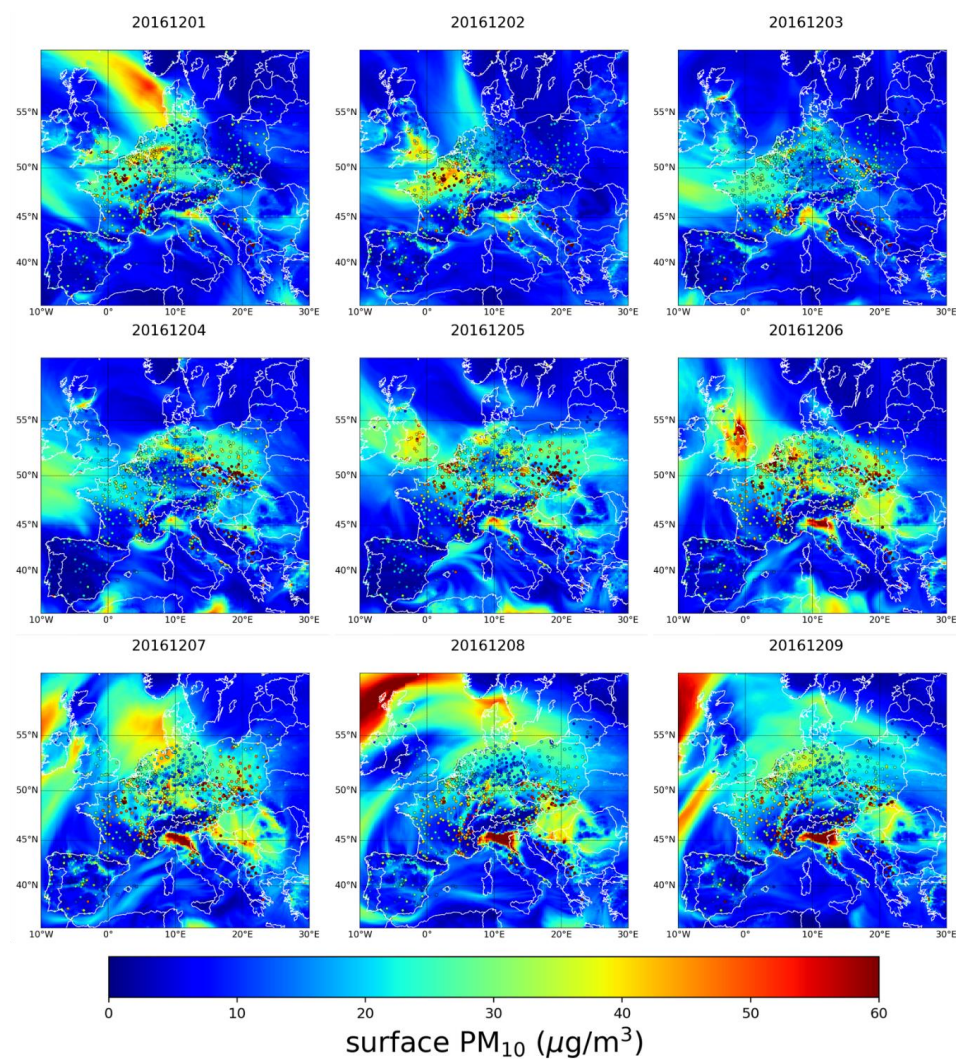
Figure 2: Daily surface PM$_{10}$ concentration in µg/m^3 over Europe predicted by the EMEP model from December 01st to 09th 2016. The colored dots correspond to the daily mean of AirBase stations (rural and urban stations).
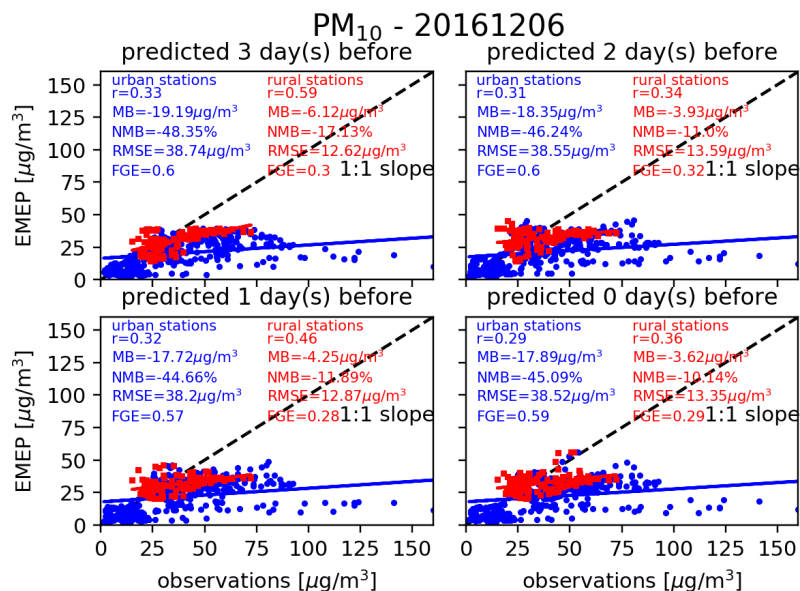
Figure 3: Scatterplot between the hourly PM$_{10}$ concentrations in µg/m^3 over all the studied cities using the 9 grids definition, predicted by the EMEP model on December 06th 2016 and the observations of the urban sites (blue dot) and rural sites (red square). For this case, there are 19 cities which have urban stations in their domain and 5 cities which have rural stations in their domain. The observations are collocated in time to the EMEP predictions and then averaged within the city edge to match the studied grid. The four panels correspond to the different predictions from 3 days before the December 06th to the actual day, i.e. December 06th. The correlation coefficient (r), the mean bias (MB), the normalized mean bias (NMB), the root-mean-square error (RMSE) and the fractional gross error (FGE) are provided on each panel. The blue and the red lines represent the linear fits.
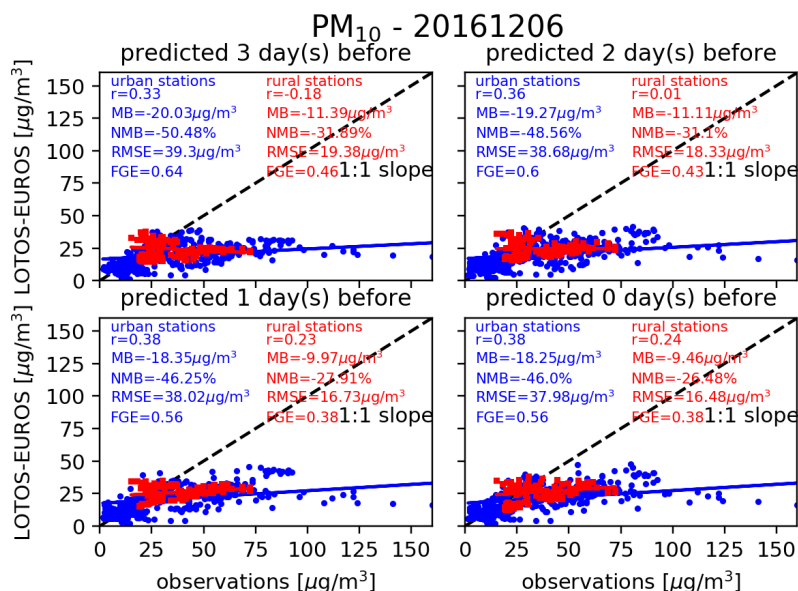
Figure 4: As Fig. 3 for LOTOS-EUROS.
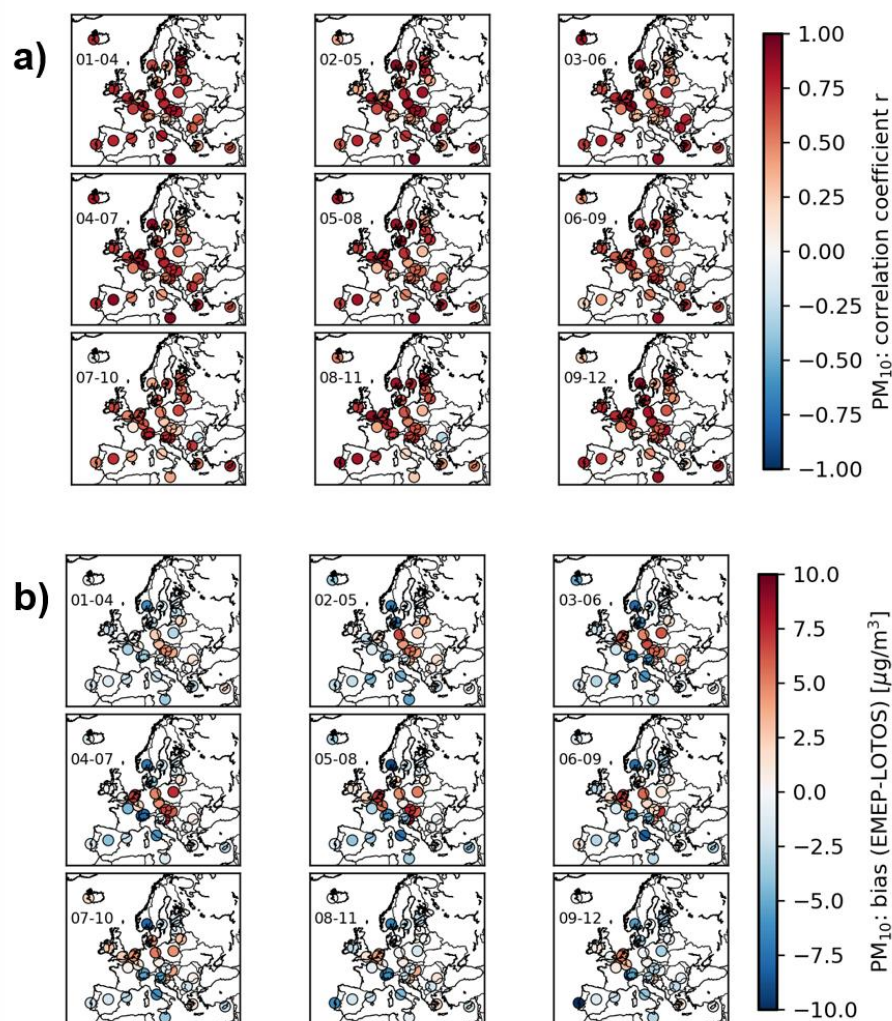
Figure 5: Correlation coefficient (a) and bias (b) in the predicted PM$_{10}$ concentrations between the EMEP model and LOTOS-EUROS over all the studied cities using the 9 grids definition for each 4day-forecast (01-04 Dec 2016, 02-05 Dec 2016, 03-06 Dec 2016, 04-07 Dec 2016, 05-08 Dec 2016, 06-09 Dec 2016, 07-10 Dec 2016, 08-11 Dec 2016, 09-12 Dec 2016).

780

785

790
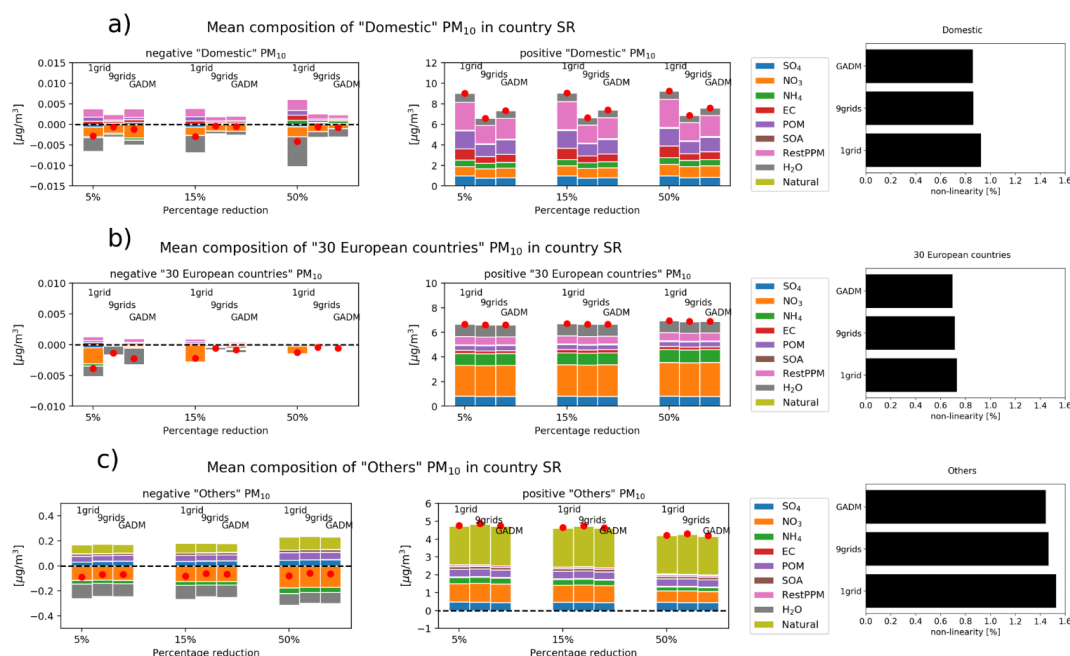
Figure 6: Mean composition of "Domestic" (a), "30 European countries" (b), and "Others" PM₁₀ split into a negative concentration (left panel) and a positive concentration (middle panel), calculated by the EMEP country SR over the 34 European cities and for each 4day-forecast. The PM₁₀ composition is highlighted with the color code. The results for the 3 city definitions (1 grid, 9 grids, GADM) and for the percentage of reduction used in the perturbation EMEP runs

795 **(5%, 15%, 50%) are shown. The "Domestic" contribution corresponds to the contribution from the domestic country to the city (e.g. from France to Paris). "30 European countries" corresponds to the other 30 European countries used in the study. "Others" gathers natural sources, the other countries included in the regional domain, the boundary conditions, the ship traffic, the biogenic sources, the soil NO emission, the aircraft emission and the lightning. The red dot represents the mean PM₁₀ concentration. The black horizontal bars (right panel) show the mean non-linearity**

800 **calculated for each contribution and for the three city definitions. The non-linearity is calculated for each hourly concentration as the standard deviation of the hourly contribution weighted by the hourly mean of the total concentration.**

805

810
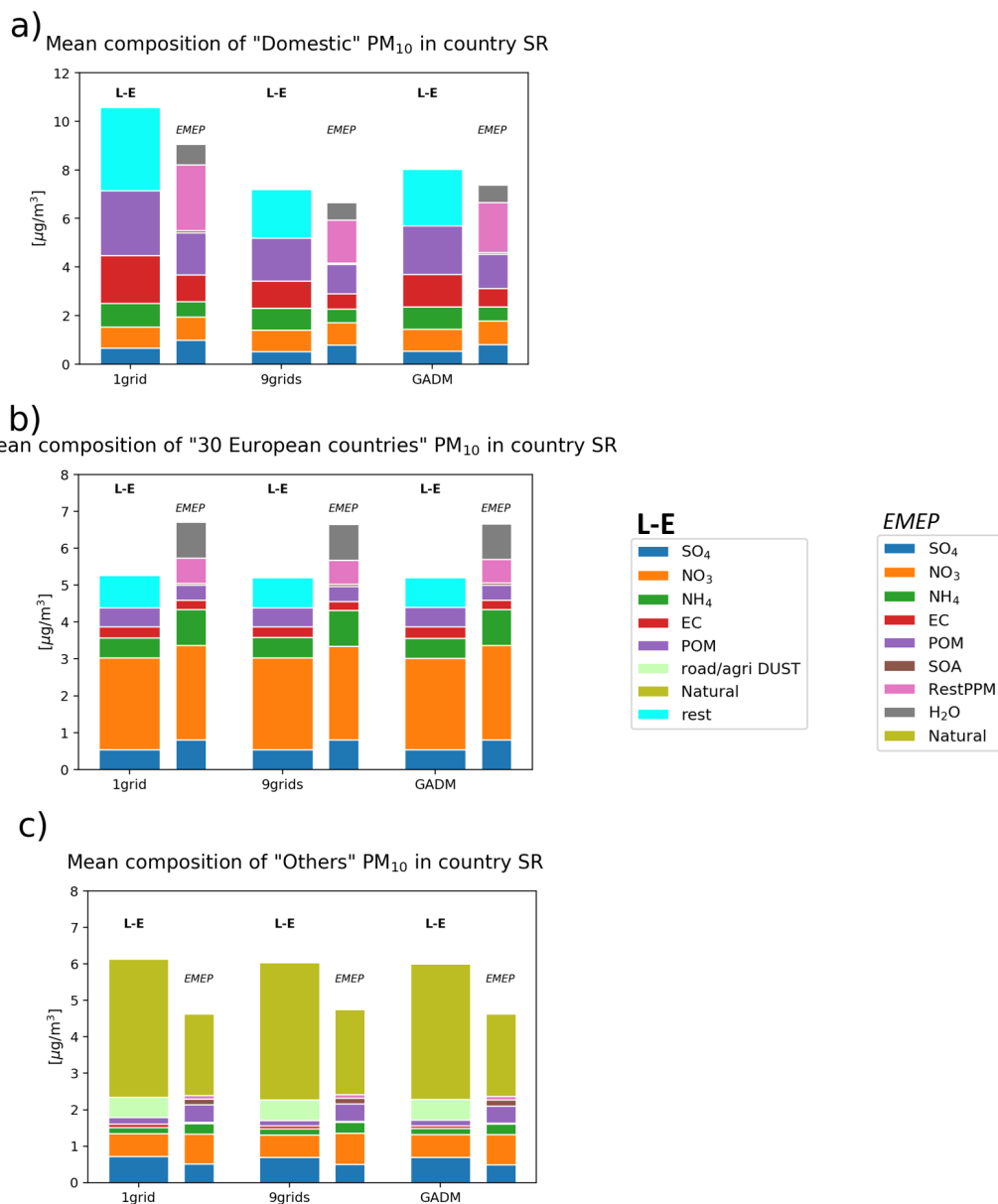
Figure 7: Mean composition of "Domestic" (a), "30 European countries" (b), and "Others" PM$_{10}$ calculated by the LOTOS-EUROS (L-E) country SR over the 34 European cities and for each 4day-forecast. The result from the EMEP country SR, by using a 15% perturbation run has also been added for comparison. The PM$_{10}$ composition is highlighted with the color code. Rest corresponds to the difference between the PM$_{10}$ and the sum of the components listed on the plot. The results for the 3 city definitions (1 grid, 9 grids, GADM) are shown. The "Domestic" contribution corresponds to the contribution from the domestic country to the city (e.g. from France to Paris). "30 European countries" corresponds to the other 30 European countries used in the study. "Others" in the LOTOS-EUROS country SR is slightly different to the EMEP "Others". "Others" in the LOTOS-EUROS country SR gathers natural sources, the other countries included in the regional domain, the boundary conditions, the dust emitted by the road traffic and agriculture, the ship traffic, the aircraft emission and the lightning.
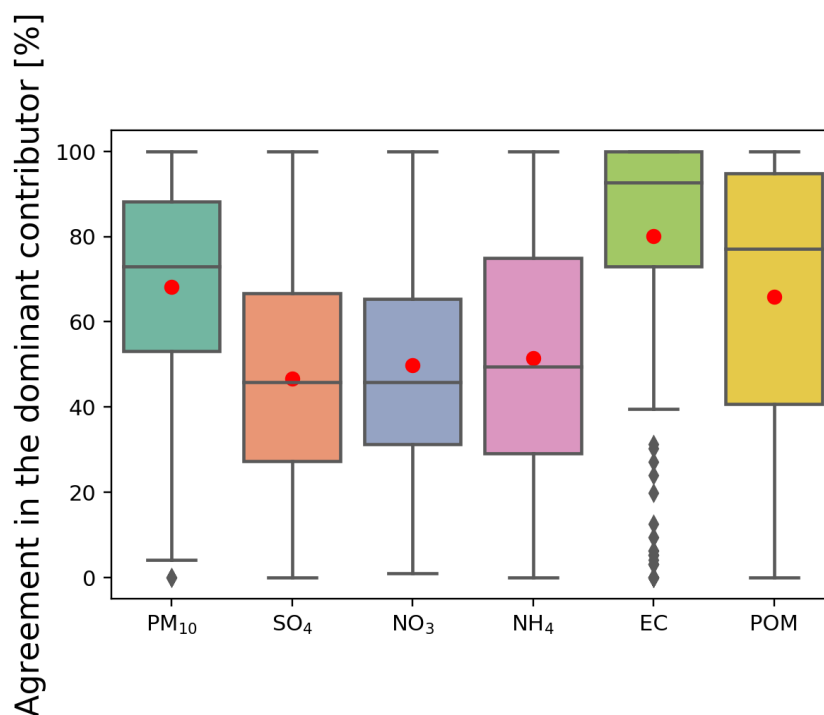
Figure 8: Agreement in the determination of the dominant country contributor for PM$_{10}$, SO$_4$, NO$_3$, NH$_4$, EC and POM in percent, determined over all the studied cities using the 9 grids definition and for all 4day-forecasts. The line that divides the box into two parts represents the median of the data. The end of the box shows the upper and lower quartiles. The extreme lines show the highest and lowest value excluding outliers which are represented by grey diamonds. The red dots correspond to the mean of each data set.

815
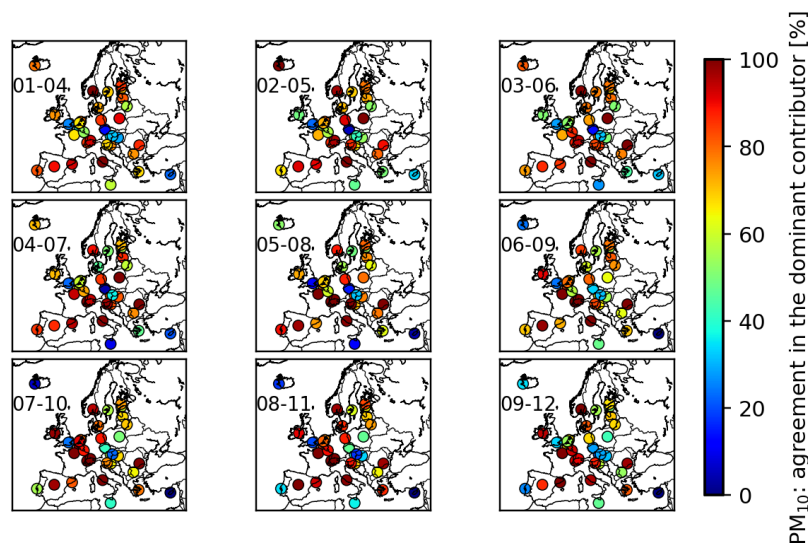
Figure 9: Agreement in the determination of the dominant country contributor for PM₁₀ in percent, and for each 4day-forecast (01-04 Dec 2016, 02-05 Dec 2016, 03-06 Dec 2016, 04-07 Dec 2016, 05-08 Dec 2016, 06-09 Dec 2016, 07-10 Dec 2016, 08-11 Dec 2016, 09-12 Dec 2016) over all the cities using the 9 grids definition.
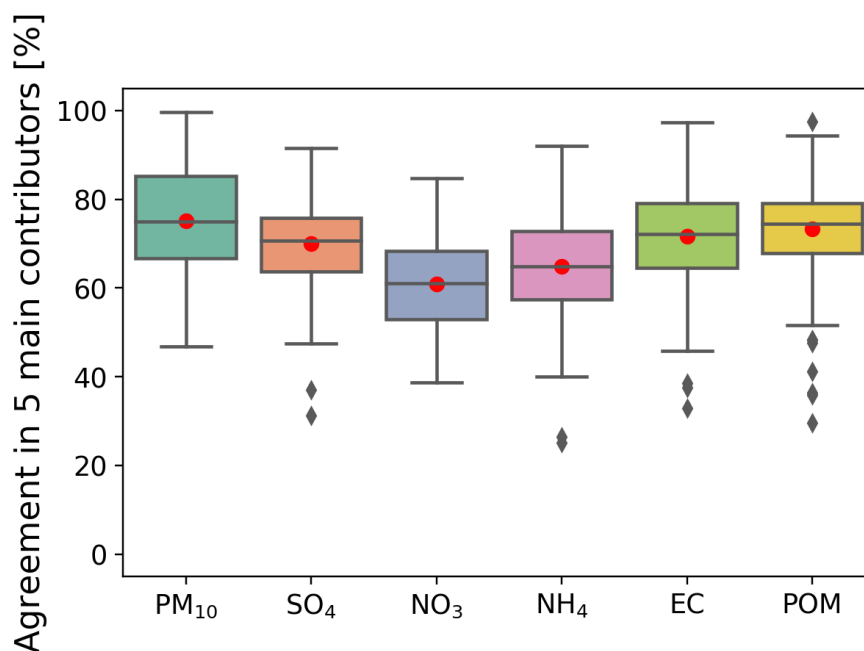
Figure 10: Agreement in the determination of the five main country contributors for PM₁₀, SO₄, NO₃, NH₄, EC and POM in percent, determined over all the studied cities using the 9 grids definition and for all 4day-forecasts. The line that divides the box into two parts represents the median of the data. The end of the box shows the upper and lower quartiles. The extreme lines show the highest and lowest value excluding outliers which are represented by grey diamonds. The red dots correspond to the mean of each data set.